Check for updates

Engineered dissipation for quantum information science

Patrick M. Harrington[1]✉, Erich J. Mueller[2]✉ and Kater W. Murch[3]✉

Abstract | Quantum information processing relies on the precise control of non-classical states in the presence of many uncontrolled environmental degrees of freedom. The interactions between the relevant degrees of freedom and the environment are often viewed as detrimental, as they dissipate energy and decohere quantum states. Nonetheless, when controlled, dissipation is an essential tool for manipulating quantum information: dissipation engineering enables quantum measurement, quantum-state preparation and quantum-state stabilization. The advances in quantum technologies, marked by improvements of characteristic coherence times and extensible architectures for quantum control, have coincided with the development of such dissipation engineering tools that interface quantum and classical degrees of freedom. This Review presents dissipation as a fundamental aspect of the measurement and control of quantum devices, and highlights the role of dissipation engineering in quantum error correction and quantum simulation.

Dissipation makes quantum information science possible. Among other things, it provides the means to measure quantum systems — driving all the paradoxical phenomena that come with entangling quantum degrees of freedom with macroscopic states. When uncontrolled, however, dissipation ruins the delicate quantum coherence at the heart of quantum information science: it reduces the fidelity of quantum gates, adds noise to measurement signals and ultimately poses a challenge to achieving the level of control necessary to harness quantum systems to gain any advantage or insight. Advances in quantum technology must contend with this dual edge to engineer dissipation. In this Review, we highlight recent experimental and theoretical advances implementing dissipation, either subtly or bluntly, to advance quantum technologies.

Dissipation engineering principles underlie all quantum information processing; any judicious choice of hardware with classical controls must account for naturally accompanying dissipation[1]. Dissipative system–environment interactions support gate operations and state readout, whereas, in turn, fluctuations of the environment impose quantum coherence limits. Engineered dissipation[2] incorporates methods that control system–environment interactions, and the environment itself, to adapt dissipative processes for tasks including quantum-state preparation[3,4], stabilization of quantum states[3,5–12], entanglement and teleportation of quantum states[13–15], the creation of decoherence-free[16] and excitation-number-conserving[17–19] subspaces, and the implementation of quantum error detection and correction[20–25]. During the present age of noisy intermediate-scale quantum (NISQ) computing[26], practical quantum information processing requires hardware-specific dissipation engineering methods to demonstrate low-error-rate devices for scalable quantum computation, simulation and sensing[27].

[1]Research Laboratory of Electronics, Massachusetts Institute of Technology, Cambridge, MA, USA.

[2]Laboratory of Atomic and Solid State Physics, Cornell University, Ithaca, NY, USA.

[3]Department of Physics, Washington University, St. Louis, MO, USA.

✉e-mail: pmh@mit.edu; em256@cornell.edu; murch@physics.wustl.edu

https://doi.org/10.1038/s42254-022-00494-8

Zeno effects and Zeno dynamics

The act of measuring a quantum system can strongly influence its dynamics. In particular, measuring a quantity can prevent it from changing. This effect has been dubbed the 'quantum Zeno effect', an allusion to Zeno of Elea's incorrect argument that an arrow, if continuously observed, should remain frozen in flight[28–30]. In the quantum Zeno effect, the quantum state is frozen by the act of repeated measurement. One can also liken it to the adage that 'a watched pot never boils'. More formally, the process of repeated measurements introduces measurement back-action, a dissipative effect in the system dynamics. In the case of Zeno effects[31,32], back-action dynamics are caused by the measurement process itself, irrespective of particular measurement results[33]. Zeno effects are not limited to systems that are explicitly being measured: dissipation can be interpreted in terms of 'measurements from the environment', and the Zeno effect is an important part of using dissipation to control quantum states.

The interplay between measurement and quantum dynamics is well illustrated by a two-level system undergoing Rabi oscillations with frequency Ω between states $|\uparrow\rangle$ and $|\downarrow\rangle$, eigenstates of the $\hat{\sigma}_z$ Pauli operator. (This was the setting of the first quantum Zeno experiment with trapped ions[30].) If the system is measured repeatedly

Key points

- Dissipation is essential for quantum information processing: resetting to the ground state, measurement and cooling all require dissipation.
- Carefully engineered dissipation can protect quantum information, control dynamics and enforce constraints.
- Dissipation finds applications in quantum error correction, quantum sensing and quantum simulation.
- Much of dissipation engineering focuses on designing 'dark' or dissipation-free manifolds of states that are stabilized by the dissipative process.

in this basis after each duration τ, the system is then randomly projected into one of the $\hat{\sigma}_z$ eigenstates. The probability p of flipping from one eigenstate to another between two successive measurements is $p = \sin^2(\Omega\tau)$. Thus the system becomes frozen in one of the $|\uparrow\rangle$ or $|\downarrow\rangle$ states when the measurement rate is large compared with the Rabi rate ($\Omega\tau \ll 1$). In a system with more coupled levels, the implications can be rich, and many dissipative control schemes that leverage measurement back-action can be interpreted through Zeno effects.

The Zeno effect is relevant for engineered dissipation when the coupling to the environment (that is, the measurement rate) is strong. This situation can suggest the paradoxical conclusion that increasing the environmental coupling can actually lead to less loss (of particles, for example), in the strong coupling limit. Consider the case where, instead of measuring our two-level system, we introduce an incoherent decay from $|\downarrow\rangle$ to $|\uparrow\rangle$, corresponding to spontaneous emission of photons with rate Γ, and described by a jump operator $\hat{L} = \sqrt{\Gamma}\,|\uparrow\rangle\langle\downarrow|$ (see BOX 1). We envision starting the system in the ground state, $|\uparrow\rangle$. When the dissipation rate is small compared with the Rabi frequency, $\Gamma \ll \Omega$, the system rapidly oscillates, and is in the unstable excited state $|\downarrow\rangle$ approximately half the time. The rate of photon emission is then $\Gamma/2$, which grows with Γ, as one would intuitively expect. Conversely, if $\Gamma \gg \Omega$, the Zeno effect freezes the system in the ground state, $|\uparrow\rangle$, and the photon emission rate scales as Ω^2/Γ: the dissipation rate actually falls with Γ. In the limit of strong dissipation ($\Gamma \to \infty$), no photons are emitted, and one can replace the dissipation with the constraint that the system can never be in $|\downarrow\rangle$, essentially freezing the dynamics in the $|\uparrow\rangle$ state. Thus, very strong dissipation can be used for coherent control, including the processing of quantum information.

One way to gain an intuitive understanding of this effect is to interpret it as a complex detuning of the transition from $|\downarrow\rangle$ to $|\uparrow\rangle$. As introduced in BOX 1, the dynamics conditioned by the absence of an dissipative event are described by a non-Hermitian effective Hamiltonian $\hat{H}_{\mathrm{eff}} = \hat{H} - \mathrm{i}\sum_\alpha \hat{L}_\alpha^\dagger \hat{L}_\alpha$, where $\hat{L}_\alpha$ are the jump operators. Here, the term $\mathrm{i}\hat{L}^\dagger\hat{L} = \mathrm{i}\Gamma|\downarrow\rangle\langle\downarrow|$ gives the excited state a complex energy. The shift of the energy from the real axis yields an effective detuning. If the detuning is large, then any coupling between $|\downarrow\rangle$ and $|\uparrow\rangle$ is far off-resonant, and the system stays in the $|\uparrow\rangle$ state.

As a simple concrete example, consider a three-level system, with states $|A\rangle, |B\rangle, |C\rangle$, and a Hamiltonian that drives transitions $A \leftrightarrow B \leftrightarrow C$ (FIG. 1a). If a very strong dissipation is added to $|C\rangle$, the system will simply undergo Rabi oscillations between $|A\rangle$ and $|B\rangle$, never transitioning to $|C\rangle$ (because the dissipation 'detunes' that level). For this driven-dissipative system, an effective ground state is formed by the subspace spanned by the states $|A\rangle$ and $|B\rangle$, while excitations out of this ground state are suppressed by the strong dissipation on $|C\rangle$. The state-selective dissipation introduces a constraint — a feature that is valuable for quantum information processing and sensing.

In this case, the space spanned by $|A\rangle$ and $|B\rangle$ is an example of a dark subspace or decoherence-free subspace[34]. Such a space exists whenever there are states in the null-space of the dissipative part of the effective Hamiltonian, $\hat{Q} = \sum_\alpha \hat{L}_\alpha^\dagger \hat{L}_\alpha$. When the dissipation is strong ($||\hat{Q}|| \gg ||\hat{H}||$), to leading order, dynamics are restricted to that subspace. Applying the standard prescription for degenerate perturbation theory, the system evolves under $\hat{H}$ projected into this dark subspace. If $\hat{H}$ and $\hat{Q}$ do not commute, the resulting Zeno dynamics can be rich[16,35–44]. The remarkable feature here is that strong dissipation can lead to non-trivial coherent evolution. The states in the dark subspace are long-lived, with lifetimes that scale inversely with the dissipation strength.

The Zeno effect provides a framework that connects measurement, environmental couplings, and the back-action dynamics from these dissipative processes. Moreover, the Zeno effect offers practical tools for quantum information processing: in atomic systems it is used to extend the lifetime of molecular states[45], tune interactions[46] and even enhance the precision of spectroscopy[47]. Dissipation from strong measurement can create decoherence-free subspaces, which can provide an essential component of quantum error correction[48,49]. The Zeno effect can even be used for quantum gates, as demonstrated by a recent experiment involving superconducting circuits[50]. In this study, two qubits with no direct interaction were entangled by using a projective measurement to confine the qubits to a particular non-local subspace, which allowed a single qubit rotation to impart a conditional phase.

Dissipative engineering toolbox

Although the Zeno effect is largely passive, there are a number of more active approaches to dissipation engineering. The classic example, illustrated in FIG. 1b, is optical pumping. Consider a three-level atom with two long-lived states $|\uparrow\rangle, |\downarrow\rangle$ and one short-lived state $|x\rangle$. The latter can decay into $|\uparrow\rangle$ by emitting a photon. To pump the system into $|\uparrow\rangle$, one turns on a drive between $|\downarrow\rangle$ and $|x\rangle$. The system will cycle between those states, eventually decaying into $|\uparrow\rangle$. If the temperature of the electromagnetic field environment is small compared with the level spacing between $|\uparrow\rangle$ and $|x\rangle$, then the decay is unidirectional; there are no thermal photons to drive the $|\uparrow\rangle \to |x\rangle$ transition, and hence $|\uparrow\rangle$ is a dark state.

This simple example highlights a key observation: dissipation can act as a one-way valve, which inevitably leads the system into a dark state or manifold. In this way, entropy is transferred from the system of interest to the bath. This approach has been applied to produce quantum states in all the forerunning platforms for quantum information processing[4,6,9–12,51–64].

A wide range of states can be produced by such pumping protocols, including ones that are highly

Box 1 | **Lindblad formalism**

A typical approach to modelling a dissipative quantum system (described by Hamiltonian $\hat{H}$) is to consider it as a subsystem of a larger environment (panel **a**). The system bath interaction involves can involve several types of interactions. In the case of decay, flipping the spin (σ_-) creates excitations in the bath $b^\dagger$, or vice versa ($\sigma_+ b$). In the case of dephasing, the energies of the bath modes depend on the state of the system. The reduced dynamics of the system is given by equations of motion for the system's density matrix $\hat{\rho}$, which plays the role of the classical phase-space distribution function. Given an ensemble of quantum states $|j\rangle$, which appear with probability p_j, the density matrix is $\hat{\rho} = \Sigma_j p_j |j\rangle\langle j|$. Under several assumptions (the Born–Markov approximation), where the environment can be treated as memoryless and decoupled from the system, the equations of motion for the density matrix have the Lindblad form[287],

$$\partial_t \hat{\rho} = \frac{1}{\mathrm{i}}[\hat{H}, \hat{\rho}] + \sum_\alpha \Gamma_\alpha \left(\hat{L}_\alpha \hat{\rho} \hat{L}_\alpha^\dagger - \frac{1}{2} \hat{L}_\alpha^\dagger \hat{L}_\alpha \hat{\rho} - \frac{1}{2} \hat{\rho} \hat{L}_\alpha^\dagger \hat{L}_\alpha \right). \tag{1}$$

The operators $\hat{L}_\alpha$, referred to as jump operators, describe the dissipation, where α indicates the different dissipation channels such as dephasing or decay for each eigenstate of H. As is clear from our formulation, the coefficients Γ_α have to be non-negative. This ensures that the system dynamics is a completely positive trace-preserving map[287]. In this context, dissipation engineering amounts to controlling the jump operators. There can be a rich interplay between the Hamiltonian term and the dissipation, particularly when the jump operators and Hamiltonian do not commute, or the Hamiltonian is time-dependent — a driven-dissipative setting.

One classifies forms of dissipation by reference to the natural basis: for a qubit this is typically the eigenstates of the $\hat{\sigma}_z$ operator, which commutes with the Hamiltonian of the bare undriven system. In this case, the density matrix is a 2×2 Hermitian matrix, and is fully characterized by the expectation values of the Pauli matrices (σ_x,σ_y,σ_z), allowing it to be visualized as a point on the Bloch sphere.

Decay involves transitions between basis states. For example, spontaneous emission corresponds to $\hat{L} \propto |\uparrow\rangle\langle\downarrow|$. As depicted in panel **b**, states evolve to a single pole of the Bloch sphere. The arrows within the Bloch sphere depict the flow of states to the $|\uparrow\rangle$ state. The red line shows an example decay trajectory initialized as a partially excited superposition on the surface of the Bloch sphere. In contrast, dephasing does not lead to transitions between basis states, but instead destroys phase-coherence. For example, a projective measurement in the energy basis corresponds to two jump operators $\hat{L}_\uparrow \propto |\uparrow\rangle\langle\uparrow|$, and $\hat{L}_\downarrow \propto |\downarrow\rangle\langle\downarrow|$. For a qubit, dephasing occurs when $\hat{L}_\alpha$ commutes with $\hat{\sigma}_z$. As depicted in panel **c**, dephasing brings the state to the $\hat{z}$ axis of the Bloch sphere without changing $\langle\hat{\sigma}_z\rangle$. The arrows show that superposition states evolve to the $\langle\sigma_z\rangle$ axis of the Bloch sphere: incoherent populations in the $\langle\sigma_z\rangle$ basis. The red line shows an example dephasing trajectory initialized on the surface of the Bloch sphere.

The term $\hat{L}_\alpha \hat{\rho} \hat{L}_\alpha^\dagger$ corresponds to applying the operator $\hat{L}_\alpha$ to every state in the ensemble: it encodes the change to the density matrix when a jump occurs. The last two terms in equation (1) represent the influence of the environment on the system in the absence of a jump. They can be combined with the coherent evolution, writing

$$\partial_t \hat{\rho} = \frac{1}{\mathrm{i}}(\hat{H}_{\text{eff}} \hat{\rho} - \hat{\rho} \hat{H}_{\text{eff}}^\dagger) + \sum_\alpha \hat{L}_\alpha \hat{\rho} \hat{L}_\alpha^\dagger. \tag{2}$$

The non-Hermitian effective Hamiltonian,

$$\hat{H}_{\text{eff}} = \hat{H} - \mathrm{i} \sum_\alpha \hat{L}_\alpha^\dagger \hat{L}_\alpha, \tag{3}$$

represents the evolution of the system conditioned on no jumps occurring[23,288,289]. The dynamics of this non-Hermitian Hamiltonian describes the reduced dynamics of the system under dissipation, and thereby encodes the Zeno effect.

entangled[9,65–76]. For example, experiments on superconducting qubits and trapped ions[51,57] engineered dissipative processes to prepare a two-qubit Bell state, $|\phi_-\rangle \propto |\uparrow\downarrow\rangle - |\downarrow\uparrow\rangle$. This is a maximally entangled state. The requisite engineering was fairly involved, taking advantage of detailed features of the hardware, but on a conceptual level it was very similar to optical pumping: whenever the system is not in the desired target state, it is subject to entangling dissipative processes.

Optical cooling provides a closely related example of dissipation engineering. One can cool motional or low-energy internal degrees of freedom by coupling mechanical oscillators[77–81], atoms/ions[82–86] or superconducting circuits[5,52] to the electromagnetic field. One needs to arrange a setting where the rate of energy-increasing processes are smaller than those of energy-decreasing processes.

Such selectivity typically comes from sculpting the density of states, or from adding extra drives that couple to short-lived states. A classic example is Raman sideband cooling of the motion of a trapped ion[87]. An optical transition drives the ion from its electronic ground state to a short-lived electronic excited state. This transition is generically accompanied by a simultaneous change in the motional wavefunction. If the drive is red-detuned, then transitions that reduce the motional energy are favoured. This can be interpreted as a form of coherent feedback[88,89].

In all these examples, aspects of the quantum state are correlated with the environment, which connects closely with modern descriptions of the process of quantum measurement where measurement is treated in a multi-step process. The interaction between the quantum system and its environment leads to changes in the environment that depend on the system's states, as sketched in FIG. 2. In this context, the environment forms 'pointer states'[90]. We use the concept of environment very generally in this case; for example, in the paradigmatic example of a Stern–Gerlach measurement, the interaction couples the electron spin states with its momentum — the momentum degree of freedom plays the role of the environment. After the interaction, a measurement of the pointer state gives information about the system state, collapsing the entanglement. At this point, the measurement results become classical information, and the effect of the interaction on the system is referred to as back-action. This approach extends the treatment of measurement beyond textbook concepts of projective measurements. Here the environment can have a much larger Hilbert space than the system (as is the case of the infinite-dimensional Hilbert space of the electron's momentum). As such, the wide range of measurement outcomes from the environment yield different partial measurements on the system. These are weak measurements[91]. The degree of measurement can vary: if the environmental states are partially overlapping (as in the central panel of FIG. 2), one only gains partial information about the quantum state[92,93]. The right-hand panel of FIG. 2 illustrates the case of a strong, or projective, measurement, where the environmental states are orthogonal[94]; any possible measurement outcome of the environment corresponds to one or the other of the systems states. The Lindblad formalism explained in BOX 1 ignores the state of the environment, so the master equation evolution is the result averaging over the ensemble of individual trajectories. However, as described in BOX 2, there are other techniques (quantum trajectories) that allow one to model the measurement outcomes and calculate the system dynamics contingent on those outcomes[91,95–99]. These are referred to as the 'unravelling' of the Lindblad master equation.

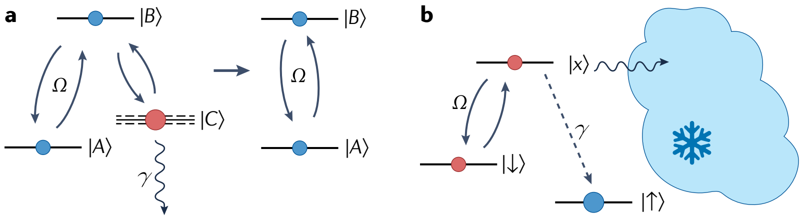

Fig. 1 | **Zeno effects and optical pumping in three-level systems. a** | The effect of strong dissipation on state $|C\rangle$ (given by rate γ) creates a decoherence-free subspace spanning the states $|A\rangle$ and $|B\rangle$ which are coupled at rate Ω. **b** | An example of optical pumping to a lower energy state $|\uparrow\rangle$ to achieve ground-state cooling. The combination of drive (Ω) and dissipation (γ) irreversibly brings the state $|\downarrow\rangle$ to $|\uparrow\rangle$, by coupling to a lossy state $|x\rangle$. Here the environment is a cold reservoir that acts as an 'entropy dump'.

Quantum measurement embodies the interplay between classical and quantum information. The integration of this classical information into a feedback circuit can alter dynamics[100], stabilizing target states of the system[101], or optimizing information that is extracted about the system[10,102,103]. The next section explores how the interplay between measurement and feedback is critical to the implementation of quantum error correction.

Applications

We now discuss different applications of dissipation engineering including quantum error correction, quantum sensing and quantum simulation.

Quantum error correction

The most important application of the quantum measurement and feedback is protecting quantum information. Typical approaches to such quantum error correction use stabilizer, or syndrome, measurements — measurements that do not disturb the logical states yet provide information that can be used to detect and correct errors. Quantum information is stored in a redundant manner, and measurements detect errors at a stage where they can still be corrected. Errors are corrected by gate operations, rotating the system back into the logical computational subspace, or the syndrome measurements are recorded and an appropriate correction is applied at the end of the computation. The measurement correction cycle is an example of engineered dissipation, precisely because the measurements (which are intrinsically dissipative) need to be engineered not to disturb the logical states. The measurement–feedback system can be implemented at a hardware level, making the system self-correcting[104–113], or other hardware choices can be made to reduce noise sensitivity[114,115]. Some of these approaches are described as autonomous error correction and involve engineered dissipation.

An illustrative example of quantum error correction is the bit-flip code[116], which embeds the logical states $|0_L\rangle$ and $|1_L\rangle$ redundantly in three qubits, $|0_L\rangle = |000\rangle$ and $|1_L\rangle = |111\rangle$. A single bit-flip error can then be detected by majority vote without revealing the individual qubit states. This is achieved with pair-wise parity measurements[12,117]. These parity measurements are the prototypical examples of stabilizers — they reveal the occurrence of individual errors, yet, because they commute with all observables of the logical qubits, do not disturb the encoded information. In the language of Zeno dynamics, the logical computational subspace is a dark subspace in the measurement process. Extensions of this simple approach, using a larger quantity of qubits and more complicated stabilizer measurements, in principle allow for arbitrary qubit errors to be corrected. Different approaches provide varying degrees of error tolerance, at the cost of physical resources. For example, detection of either bit-flip or phase-flip errors with repetition codes has demonstrated the suppression of logical error rates and favourable scaling on 21 qubits with 50 rounds of quantum error detection[24]. The surface code has been proposed as a practical approach to large-scale quantum computation[118], tolerating single-qubit error rates comparable to current experimental limits[20,119] and scalable with current qubit architectures[120]. With present error rates, however, the surface code would still require thousands of physical qubits per logical qubit, making the realization of a fault-tolerant error-corrected quantum processor a still-distant experimental goal.

Rather than encode quantum information redundantly in multiple qubits, an alternative approach is to use the infinite-dimensional Hilbert space of a harmonic oscillator (for example, a single mode of a microwave cavity) to realize logical qubits[121]. The simplest of these bosonic codes are binomial codes, which encode qubits in a finite number of Fock states, $\{|n\rangle\}$, each of which has a fixed number of quanta[122,123]. The coefficients of the Fock states are related to binomial coefficients, with a simple example having $|0_L\rangle \propto |0\rangle + |4\rangle$, $|1_L\rangle = |2\rangle$ as logical qubits. This encoding is chosen so that every logical state has the same parity, such that the loss of a photon, which is the dominant error process for oscillator states, can be detected by measuring parity. Then a unitary operation can correct the error without scrambling the quantum information.

Similarly, bosonic cat codes[22,104,110,124–127] are robust against single-photon loss by encoding logical qubits in Schrödinger cat states — superpositions of two or more coherent states. Using this architecture, with real-time measurement and feedback, a logical qubit lifetime longer than the relaxation time of its constituent parts was demonstrated[128]. As a coherent state of an oscillator can be maintained in steady state via a combination of dissipation and resonant driving, the cat states can be stabilized by appropriate two-photon driving and dissipation[8,129]. In this way, dissipation can be harnessed to actually reduce error rates, beyond just detecting errors for correction. Extending the approach taken in such cat codes, the Gottesman–Kitaev–Preskill (GKP) error-correcting code[130] encodes logical qubits in a periodic grid in the phase space of a harmonic oscillator. The GKP encoding is non-local for all three Pauli operators, meaning that small perturbations, entering as small phase-space displacements of the oscillator, can be corrected. In circuit quantum electrodynamics, the GKP code has been implemented by creating oscillator displacements conditional on a qubit state in such a way that measurement of the qubit projects the oscillator onto the desired grid state[131]. The GKP state has also been produced using the motional degrees of freedom of trapped ions[112,132].

These examples can all be viewed as digital approaches to error correction, where the evolution is broken into discrete blocks interrupted by stabilizer measurements and feedback. Complementary to this approach is the use of continuous measurement to detect errors[133], as highlighted in an experiment where errors, which take the form of quantum jumps out of a desired space, are detected and corrected through continuous measurement and feedback[134]. In this experiment, a circuit supporting three quantum levels has one pair of levels that are 'bright' and one state that is 'dark'. Quantum jumps can take the system out of the bright manifold of states, but continuous monitoring can detect the jumps, enabling a feedback correction to reverse the quantum jump before it is complete. This feedback correction works because the quantum jumps, despite occurring stochastically, correspond to a measurement-driven evolution that is coherent. This is because the measurement signals associated with these jumps — darkness — are uniform rather than stochastic. Thus, a feedback controller, detecting only a few instances of dark signal, can apply a rotation to return the three-level system to the bright manifold; the error is corrected even before it has a chance to completely occur.

Error correction fights fire with fire: it uses one form of dissipation (measurement) to control unwanted forms of dissipation. When judiciously chosen, the additional dissipation does not disturb the encoded information, but the information gleaned allows a classical controller to compensate for the uncontrolled dissipation.

Quantum sensing

Quantum mechanics can offer advantages over classical measurement approaches for sensing. First, quantum systems are small, which gives access to smaller length scales and boosts sensitivity: the individual energy levels can be sensitive to very weak perturbations. Second, the coherent evolution of a quantum system means that it accumulates phase in proportion to a perturbation of interest, leading to higher precision. Finally, quantum entangled states offer opportunities for reduced noise and enhanced sensitivity[135].

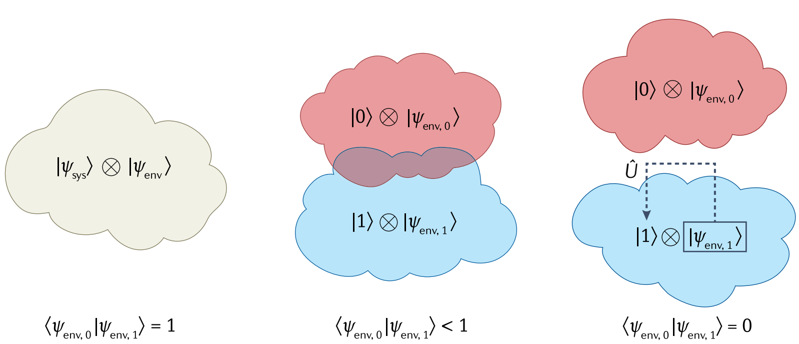

Fig. 2 | **Pointer states in quantum measurement.** Quantum measurement involves the creation of correlations between a quantum system (ψ_{sys}) and an auxiliary 'environment' (ψ_{env}), indicated here as cloud shapes. The strength of the measurement is dictated by the overlap of the these environment 'pointer' states. The central panel corresponds to a weak measurement, where the environmental outcomes are weakly correlated with the quantum state. In addition to illustrating a strong measurement, the right-hand panel depicts feedback, where the evolution of the system (quantified by the operator $\hat{U}$) is contingent on a certain measurement result.

Typically, one characterizes the performance of a quantum sensor in terms of the quantum Fisher information that can be obtained about a parameter — loosely speaking — quantifying how the distance between two quantum states depends on the sensing parameter of interest (FIG. 3a). In this sense, dissipation, which tends to create mixed states and therefore reduce the distance between states, hinders the performance of quantum sensors. Indeed, many protocols for sensing use specific (dynamical decoupling) pulses to reduce dissipative effects, while enhancing the desired accumulated phase. Alternatively, error correction approaches can be used to maintain coherent evolution, as is also required in quantum processors. There are, however, some cases where dissipation is an essential aspect of quantum sensing.

A key approach, often used in quantum sensing using nitrogen-vacancy colour centres in diamond[136,137], is to engineer a situation where the signal is encoded in the dissipation rate. As shown in FIG. 3b, these colour centres have spin sublevels (labelled with quantum numbers m_s) with splittings denoted by Δ and $2g\mu_B B_{\|}$: Δ is the zero-field splitting, and $B_{\|}$ is the component of the magnetic field along the quantization axis. The transitions from $m_s = 0$ to the other sublevels are in the microwave frequency range; magnetic field noise resonant with these transitions induces quantum jumps between them. The dissipation rate can therefore be used as a sensitive probe of such magnetic field noise. Recent work used this principle to measure the Johnson noise at nanometre resolution in normal metal films[138].

Another application where the spin dissipation can be used as a sensitive probe is in the study of many-body spin dynamics. An experiment examined how the polarization of a nitrogen-vacancy centre can diffuse through interactions with neighbouring spins[139]. The resulting power-law decay of polarization gave information that was not accessible through classical probes.

The most common mode of operation for a quantum sensor involves initializing the device, allowing it to evolve and then measuring it. An alternative approach is to probe the quantum system continuously, leading to a trade-off between the continuous accumulation of information and quantum coherent evolution. When the balance of these two effects is carefully engineered, the resulting driven-dissipative evolution can yield a powerful sensor as detailed below.

A clear example of this balance is demonstrated by dispersive detection of number parity of single electron charges that have crossed the Josephson junction — a sensor that is well suited to detect the very quasiparticle dynamics that induce relaxation in quantum processors[140]. The dispersive readout of charge-parity relies on the dissipative process of single-shot measurement to detect the system's occupation of energy eigenstates with even or odd charge-parity.

The measurement can be quantum non-demolition[141,142]: the system Hamiltonian commutes with the measurement jump operators that cause back-action dynamics. Consequently, dispersive readout ensures that the dissipation does not deleteriously alter the mapping between charge-parity and the readout signal throughout the measurement process. As such, the continuous

Box 2 | **Quantum trajectories**

The Lindblad master equation in BOX 1 models the evolution of the system's density matrix when the state of the environment is ignored — instead, the state of the environment is traced over. One may, however, wish to describe dynamics that depend on the state of the environment. As a concrete example, consider an atom that is in a superposition of its ground and excited states. If one detects a photon emerging from the atom between time t and $t+\delta t$, then the density matrix evolves as

$$\hat{\rho}^{\text{click}}_{t+\delta t} = \frac{\hat{K}_{\text{click}}\rho_t\hat{K}^{\dagger}_{\text{click}}}{\mathrm{Tr}\left[\hat{K}_{\text{click}}\hat{\rho}_t\hat{K}^{\dagger}_{\text{click}}\right]}, \tag{4}$$

where $\hat{K}_{\text{click}} = \sqrt{\gamma\,\delta t}\,|\downarrow\rangle\langle\uparrow|$ is the Kraus operator, which corresponds to the emission of a photon[290], where γ is the radiative decay rate. Conversely, if no photon is detected, the state evolves via the analogue of equation (4), but with the operator $\hat{K}_{\text{no-click}} = |\uparrow\rangle\langle\uparrow| + \sqrt{1-\gamma\,\delta t}\,|\downarrow\rangle\langle\downarrow|$. In general, there are many possible outcomes, indexed by m, with Kraus operators $\hat{K}_m$. The probability of outcome m is $P(m) = \mathrm{Tr}[\hat{K}_m\rho\hat{K}^{\dagger}_m]$, and $\sum_m \hat{K}^{\dagger}_m\hat{K}_m = 1$. If one averages over all possibilities, one recovers a Lindblad equation with jump operators $\hat{L}_m = \hat{K}_m/\sqrt{\delta t}$. By following individual trajectories, one can model both the evolution of a quantum device and the entire history of the interactions with the environment, or model the quantum dynamics conditioned on certain measurement results. Such considerations are essential for filtering, post-selection and real-time quantum feedback.

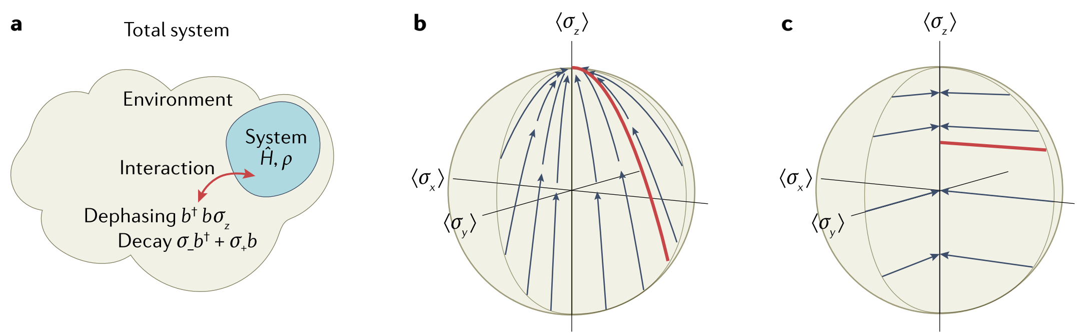

monitoring of charge-parity allows the monitoring of other quasiparticle-induced loss that can limit the coherence of superconducting qubits.

As another example, driven-dissipative evolution can be used for low-frequency magnetic field detection[143]. In this case, again using nitrogen-vacancy centres, the optical illumination that initiates and reads out the magnetic state of the colour centre is always on, creating continuous dissipation to the $|m_s = 0\rangle$ sublevel. The combination of this dissipation and an additional microwave drive that couples the magnetic sublevels yields a fluorescence intensity that is proportional to the signal of interest. The advantage here is that the sensitivity can be pushed to very low frequencies, circumventing limits posed by the intrinsic coherence of the colour centre.

The approach using continuous measurement during sensing can also be applied at the level of single quantum trajectories for a single quantum system[99,144,145]. In this case, a continuous measurement signal can be used to track a quantum system while also gaining information about the parameters of the system's Hamiltonian. This situation highlights the difference between quantum measurement (pertaining to quantum observables) and quantum sensing (pertaining to estimating parameters of a system's Hamiltonian).

Quantum simulation

Quantum simulation[146–153] refers the use of one quantum system to emulate the physics of another[154–157]: neutral atoms trapped in optical lattices as electrons in the crystal lattices of solid-state materials, superconducting circuits act as optical cavities, and atomic Rydberg excitations act as spins[158–160]. These platforms introduce new ways of studying physics and phenomena that occur on otherwise inaccessible length scales or timescales.

The same tools that are used for emulation can also be used to create new artificial systems that have no realization in nature. For example, experiments with superconducting circuits have simulated the behaviour of electrons in a hyperbolic geometry[161]. Of particular current interest is the exploration of strongly coupled models, which are not easy to study with conventional computational tools[162–164].

Quantum simulation has numerous near-term applications in physics, engineering, chemistry[165–167] and biology[168], for which quantum devices can be tailor-made to emulate a problem of interest. Engineered dissipation offers convenient methods to control many degrees of freedom and can be an important tool for quantum simulations[169].

The scope of quantum simulation goes beyond faithful replication: the analogue system may be engineered to have all properties of the original system or just a subset of those properties. For example, dissipative approaches to replicating the ground state of a Hamiltonian may fail to capture the excitation spectrum or more general dynamical aspects[170–172]. Such narrowing of the scope of a simulator can help to disentangle complicated phenomena or improve the robustness of its operation. Furthermore, these simulators can become objects of study in themselves, independent of the original motivation.

Although quantum simulation can involve 'digital' approaches where the simulation is performed using gates on a quantum computer, engineered dissipation is most relevant for analogue (or hybrid) approaches, where the degrees of freedom of the system of interest can map directly onto those of the physical hardware[173]. For analogue quantum simulation, dissipation engineering has several uses. First, dissipation can be used to constrain Hilbert spaces. Such constraints are particularly important if the analogue system has different degrees of freedom from the system of interest. Second, dissipation can be used to steer quantum simulators into states of interest[174]. The simplest example of this is cooling, but there also exist protocols in which the dissipation is engineered to pump the system into a particular excited state[175]. These same tools are also useful for annealing-based computational strategies[176]. Third, engineered dissipation is necessary for studying explicitly dissipative phenomena, such as transport in many-body systems. In the next subsections, we overview the state of the art in each of these three areas. Importantly, the quantum simulation of many-body systems with dissipative phenomena is largely unexplored in both theory and experiment, and holds promise for exploring new physics of condensed matter systems[163,164].

Constraining degrees of freedom. In practice, Zeno effects, where measuring a quantity prevents it from changing, are often complemented by some sort of coherent feedback that can be used to impose constraints to realize an effective Hamiltonian for quantum simulation. To illustrate the usefulness of dissipation for implementing constraints, consider ongoing attempts to produce cold atom analogues of the fractional quantum Hall[177] state known as the 'Pfaffian' state[178]. This is a topologically ordered state, first discussed in the context of the fractional quantum Hall effect of two-dimensional (2D) electrons in large magnetic fields, confined to two-dimensions[177]. It supports Majorana fermion excitations, and is the exact ground state of a model Hamiltonian with extremely strong short-range three-body interactions. Thus a key step in producing this state is to engineer a strong three-body repulsion (FIG. 4a). Producing such many-particle interactions is challenging. Nonetheless, it is straightforward to create a strong three-body loss term[179,180], for example by tuning near a scattering resonance. As emphasized in the first section, if this three-body loss is strong enough, the Zeno effect will restrict the system to the desired manifold, where three particles never come near each other (see FIG. 4a). In the presence of an appropriately tuned gauge field, the ground state with this constraint is the desired Pfaffian. Beyond this example of state preparation, the behaviour of systems with strong three-body losses can be quite rich[181–185].

More generally, one can add a constraint by inducing large loss: large two-body loss induces a strong effective two-body interaction[186–189]; large three-body loss induces a strong effective three-body interaction. Variants of this idea have been explored in contexts ranging from implementing magnetic models[190] to simulating gauge theories[191–193]. The more sophisticated versions of this strategy involve engineering the dissipation so that it actively pumps the system into the constrained space: this can be either through an autonomous feedback scheme or through an active approach involving measurements and correction. The states that satisfy the constraint become part of a dark-state manifold.

An important application is the use of dissipation to constrain the particle number. This allows one to emulate the behaviour of systems with particle-number conservation, such as atoms or electrons, with entities whose numbers are not conserved, such as photons or phonons. For example, the behaviour of atoms in an optical lattice can be emulated by the photonic excitations of superconducting circuits[150,194]. In this context, one wants to find a dissipation mechanism that 'measures' the number of photons such that the excitation number is stabilized: injecting more if the number is below the target, or removing excitations if the number is too large. In the language of statistical mechanics, one can think of this as creating an environment with a finite chemical potential for photonic excitations.

Several dissipative schemes have been proposed to produce an effective chemical potential for photonic excitations. The most direct approach has been implemented in experiments where the excitations of dye molecules are used as photon bath[195]. There are also strategies involving parametrically oscillating the coupling between a photonic system and its bath[196]. One of the most important insights is that it often suffices to apply the stabilization locally at only a single discrete location — as long as the excitations are sufficiently mobile, fixing the density locally will fix the average atom number.

This insight is illustrated by an experiment that reports the autonomous stabilization of a 'Mott insulator' in a superconducting circuit (see FIG. 4b) consisting of eight anharmonic quantum oscillators (transmons) coupled to each-other and microwave readout resonators[18].

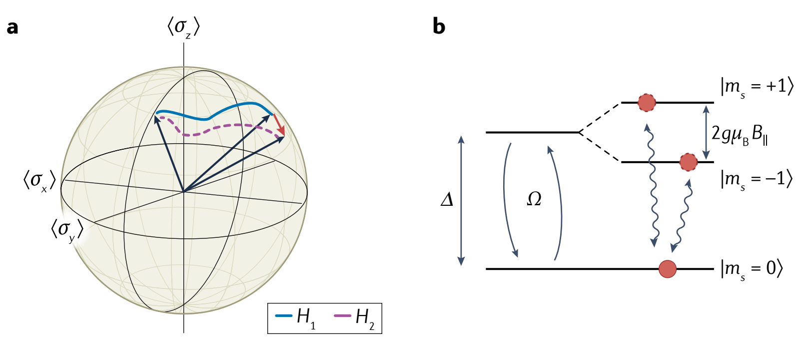

Fig. 3 | **Quantum sensing. a** | In quantum sensing, one determines the parameters that distinguish two different Hamiltonians H_1 and H_2 through distance between the final states after some time evolution. The figure illustrates this process for a single quantum spin, whose state is quantified by the expectation value of the Pauli matrices $\langle\sigma_x\rangle$, $\langle\sigma_y\rangle$, $\langle\sigma_z\rangle$. The sensitivity to the parameters is quantified by the quantum Fisher information[285,286]. **b** | Nitrogen-vacancy colour centres in diamond have optically initializable and readable magnetic sublevels (m_s) that are particularly suited to sensing. Magnetic field noise induces dissipative transitions between sublevels, making the colour centre a sensitive spectrometer. The zero-field splitting Δ is intrinsic to the material, whereas the splitting between the $m_s = \pm 1$ states is controlled by the magnetic field. Transitions between the states can be driven by a coherent drive (Ω) or magnetic field noise (blue squiggly arrows). Here, μ_B is the Bohr magneton, g is the gyromagnetic ratio and $B_\parallel$ is the external field.

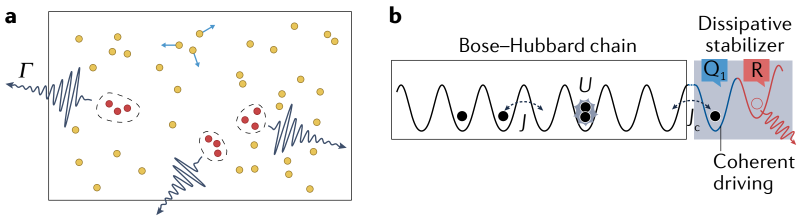

Fig. 4 | **Dissipation in quantum simulation. a** | An ensemble of molecules has an effective three-body repulsion (light blue arrows) as a consequence of strong three-body loss (dark squiggly arrows). **b** | The dissipative stabilization of a Mott insulator state, with one particle per site, where Q_1 indicates the initial qubit site of the chain and R the reservoir site, J is the nearest-neighbour tunnelling rate, U is the on-site interaction, and J_c is the tunnelling rate to the dissipative stabilizer site. The particle number is a conserved quantity in the effective ground state owing to energy-selective dissipation and the incompressibility of the Mott insulator state. Panel **b** is adapted from REF.[18], Springer Nature Ltd.

The number of quanta on each device is analogous to the number of particles on a site — and the goal is to have exactly one particle on each site (which is the defining feature of an ideal Mott insulator). The site at one end, denoted Q_1, is coupled to a 'cold reservoir' realized by a lossy resonator denoted as R. The end-site Q_1 is driven such that it is forced into a configuration with exactly one excitation. Given the ability of the excitations to hop between sites, the configuration with one particle per site is a dark state. If there is a particle 'hole', or lack of an on-site excitation, then excitations will propagate until the hole travels to Q_1, where it will be removed. The advantage of introducing local dissipation at a single site is that it is both easier to implement and leaves an unperturbed 'bulk'. However, the disadvantage is that the time it takes to remove a hole grows with the system size; excitations out of the engineered ground state may not be strongly suppressed.

This example of single-site dissipation highlights the importance of spatial structure. In many cases, the most easily implemented dissipation elements are local, which introduces some constraints on the type of states one can create. There are many examples in the literature of ideas for producing matrix product states or pair entangled states[60,197–199], including condensates, η-condensates, pair condensates and dimerized phases[175,200–202]. Because of their topical nature, particular efforts have been made to come up with approaches to produce states that either exhibit topological order or have topologically non-trivial band-structure[47,201,203–208]. Despite the dissipation being local, these systems exhibit globally conserved quantities. There are analogies between these non-local degrees of freedom and the protected logical qubits of quantum error-correcting codes[209]. Generically, the strategies of using dissipation to induce constraints have parallels in quantum error correction: the typical measurements–correction cycle can be interpreted as a dissipative process that constrains the computer to a chosen code-space.

In principle, any thermodynamic quantity can be constrained by using similar techniques to those of the Mott insulator experiment. Dissipation can introduce an effective chemical potential, and analogous approaches would correspond to the appropriate conjugate variable: for example, constraining the total spin of a system would introduce an effective magnetic field.

Simulating dissipative systems. In addition to being a tool for implementing constraints and projecting into desired states, engineered dissipation can be used to emulate and study exotic dynamics of open quantum dynamical systems. One important class of such studies is the imitation of thermal baths or reservoirs. Thermal ensembles have obvious physical importance, and they are used in numerical algorithms such as optimization[210] and machine learning[211]. A straightforward way to simulate a thermal system is to directly implement a large reservoir with many degrees of freedom[212–214]. This is resource-intensive, which has motivated approaches in which a small number of driven lossy degrees of freedom leads to a thermal ensemble[215–221]. The governing principle in engineering these artificial thermal baths is the same as used for numerical calculations: a steady-state Boltzmann distribution will be found if the detailed balance condition is satisfied, that is, the rate for transitioning from state i to state j, $P_{i\to j}$, is related to the reverse rate by the energies of the two states: $P_{i\to j}/P_{j\to i} = e^{\beta(E_i - E_j)}$, where $1/\beta = k_B T$. We emphasize that this condition must be engineered, and a generic dissipative system will not satisfy detailed balance. Examples that use this principle include coupling superconducting qubits to lossy driven microwave resonators[215] or driven lossy qubits[216]. Traditional optical cooling techniques can be considered as special cases[222–226]. Note that the resulting steady-state properties from these approaches will be universal, but the way the system approaches equilibrium will depend on the details of the reservoir and couplings. There are, however, strategies for emulating generic Lindblad equations, which can fully model the equilibration process[227–231]. The thermal baths engineered with these techniques can have a range of tunable parameters: one can engineer how they couple to the system, the spectral density of states and the extent to which information can be stored in the reservoir[232,233].

The most novel studies involve emulating non-thermal open quantum systems — largely with the goal of observing new phenomena. This includes a range of exotic non-equilibrium phases[234–236] and non-equilibrium analogues of equilibrium phase transitions[183,200,237–245]. These open quantum systems are as rich as classical dynamical systems, including limit cycles, period doubling[246–248] and all of the complexity that is found in actively driven[249] and even in living systems[250]. They also show purely quantum phenomena, such as collapses and revivals[232]. This richness of behaviour can be used in reservoir quantum computing[251,252], where dissipation is valuable for its contribution to the fading-memory property[253].

The above examples illustrate the value of quantum simulation, where one makes use of the controllability of one quantum technology to peer into systems that are more difficult to probe. In this endeavour, dissipation provides a range of techniques to adapt one type of quantum system to the physics contained in a desired Hamiltonian.

Outlook

Over the past decades, progress in quantum technologies has been marked by increasing control, particularly regarding the strength and nature of the coupling to the environment. This has led to fundamental advances in quantum science. This Review has focused on cases in which deliberate coupling to the environment yields substantial advantages. Such an approach may appear counter-intuitive at first, as one might expect coupling to an environment to increase a system's entropy. Indeed, much of the progress in quantum information processing has been due to reducing coupling to uncontrolled degrees of freedom in the environment[254–256]. Nonetheless, judicious engineering of an environment can reduce a system's entropy. There are several divergent strategies: in some cases, the environment is effectively very cold, as with the example of optical cooling, and hence acts as an entropy dump. In other cases, such as when a system is being continually measured, the environment formally takes the form of an infinite temperature bath. The information gained from the measurements, however, can be used to reduce the entropy. The prime example of this approach is quantum error correction.

Dissipation also provides new mechanisms for coherent control. An overarching strategy is provided by the quantum Zeno effect, where strong dissipation imposes constraints on the system dynamics. This can be interpreted in terms of detuning the system's eigenenergies on the complex plane, leading to Zeno effects and Zeno dynamics within a protected subspace. Even more control can be achieved with autonomous feedback, where the addition of coherent driving can funnel states into a protected subspace.

Although this Review has largely focused on practical issues, newfound capabilities to engineer many-body quantum system systems has motivated further exploration of these fundamental concepts. The first of these is quantum thermodynamics, which is an emerging field of physics in which concepts in quantum information are united with thermodynamic principles such as entropy, heat and work[257,258]. Quantum thermodynamics provides a framework to further understand and engineer dissipation.

Similarly, there is considerable progress in quantum dynamical systems[259]. These differ from their classical counterparts not only owing to the structure of the underlying microscopic equations, but also owing to the importance of quantum entanglement[260–262]. Deep insights are being developed into the connections between classical and quantum chaos[263], how information propagates in a quantum system[264], and the interplay between coherent and incoherent processes in the propagation of entanglement[265,266]. There are new dynamical phase transitions with universal critical behaviour[239,267–269]. Finally, at the intersection of quantum dynamical systems and quantum thermodynamics are questions about equilibration, when quantum systems can be described thermodynamically[270–273], and quantifying the information complexity of such systems[274,275]. The developments that are enabling quantum computation have not only presented these questions, but also offer new tools to explore them experimentally.

Techniques for modelling the dynamics of open quantum systems are continually evolving. Frontiers include techniques using tensor networks[198,276,277] or neural networks[278–282]. A difficult challenge is going beyond the Markov and Born approximations that were at the heart of much of our discussion[283,284]. The bath is not necessarily weakly coupled to the system; it can act as a memory, which is entangled with the system in non-trivial ways. If mastered, this complexity can become a resource for quantum computation and beyond.

It is clear that engineered dissipation is a key part of the technology of quantum information science. The importance of these concepts will only grow over the coming years.

Published online 18 August 2022

1. Callen, H. B. & Welton, T. A. Irreversibility and generalized noise. *Phys. Rev.* **83**, 34–40 (1951).
2. Poyatos, J. F., Cirac, J. I. & Zoller, P. Quantum reservoir engineering with laser cooled trapped ions. *Phys. Rev. Lett.* **77**, 4728–4731 (1996).
3. Boutin, S., Andersen, C. K., Venkatraman, J., Ferris, A. J. & Blais, A. Resonator reset in circuit QED by optimal control for large open quantum systems. *Phys. Rev. A* **96**, 042315 (2017).
4. Magnard, P. et al. Fast and unconditional all-microwave reset of a superconducting qubit. *Phys. Rev. Lett.* **121**, 060502 (2018).
5. Valenzuela, S. O. et al. Microwave-induced cooling of a superconducting qubit. *Science* **314**, 1589–1592 (2006).
6. Geerlings, K. et al. Demonstrating a driven reset protocol for a superconducting qubit. *Phys. Rev. Lett.* **110**, 120501 (2013).
7. Holland, E. T. et al. Single-photon-resolved cross-Kerr interaction for autonomous stabilization of photon-number states. *Phys. Rev. Lett.* **115**, 180501 (2015).
8. Leghtas, Z. et al. Confining the state of light to a quantum manifold by engineered two-photon loss. *Science* **347**, 853–857 (2015).
9. Kimchi-Schwartz, M. E. et al. Stabilizing entanglement via symmetry-selective bath engineering in superconducting qubits. *Phys. Rev. Lett.* **116**, 240503 (2016).
10. Liu, Y. et al. Comparing and combining measurement-based and driven-dissipative entanglement stabilization. *Phys. Rev. X* **6**, 011022 (2016).
11. Lu, Y. et al. Universal stabilization of a parametrically coupled qubit. *Phys. Rev. Lett.* **119**, 150502 (2017).
12. Andersen, C. K. et al. Entanglement stabilization using ancilla-based parity detection and real-time feedback in superconducting circuits. *NPJ Quantum Inf.* **5**, 69 (2019).
13. Bose, S., Knight, P. L., Plenio, M. B. & Vedral, V. Proposal for teleportation of an atomic state via cavity decay. *Phys. Rev. Lett.* **83**, 5158–5161 (1999).
14. Browne, D. E., Plenio, M. B. & Huelga, S. F. Robust creation of entanglement between ions in spatially separate cavities. *Phys. Rev. Lett.* **91**, 067901 (2003).
15. Sørensen, A. S. & Mølmer, K. Measurement induced entanglement and quantum computation with atoms in optical cavities. *Phys. Rev. Lett.* **91**, 097905 (2003).
16. Bretheau, L., Campagne-Ibarcq, P., Flurin, E., Mallet, F. & Huard, B. Quantum dynamics of an electromagnetic mode that cannot contain *N* photons. *Science* **348**, 776–779 (2015).
17. Hacohen-Gourgy, S., Ramasesh, V. V., De Grandi, C., Siddiqi, I. & Girvin, S. M. Cooling and autonomous feedback in a Bose–Hubbard chain with attractive interactions. *Phys. Rev. Lett.* **115**, 240501 (2015).
18. Ma, R. et al. A dissipatively stabilized Mott insulator of photons. *Nature* **566**, 51–57 (2019).
19. Yanay, Y., Braumüller, J., Gustavsson, S., Oliver, W. D. & Tahan, C. Two-dimensional hard-core Bose–Hubbard model with superconducting qubits. *NPJ Quantum Inf.* **6**, 58 (2020).
20. Andersen, C. K. et al. Repeated quantum error detection in a surface code. *Nat. Phys*. https://doi.org/10.1038/s41567-020-0920-y (2020).
21. Kapit, E. The upside of noise: engineered dissipation as a resource in superconducting circuits. *Quantum Sci. Technol.* **2**, 033002 (2017).
22. Leghtas, Z. et al. Hardware-efficient autonomous quantum memory protection. *Phys. Rev. Lett.* **111**, 120501 (2013).
23. Touzard, S. et al. Coherent oscillations inside a quantum manifold stabilized by dissipation. *Phys. Rev. X* **8**, 021005 (2018).
24. Chen, Z. et al. Exponential suppression of bit or phase errors with cyclic error correction. *Nature* **595**, 383–387 (2021).
25. Krinner, S. et al. Realizing repeated quantum error correction in a distance-three surface code. *Nature* **605**, 669–674 (2022).
26. Preskill, J. Quantum computing in the NISQ era and beyond. *Quantum* **2**, 79 (2018).
27. Altman, E. et al. Quantum simulators: architectures and opportunities. *PRX Quantum* **2**, 017003 (2021).
28. Degasperis, A., Fonda, L. & Ghirardi, G. C. Does the lifetime of an unstable system depend on the measuring apparatus? *Nuovo Cim. A* **21**, 471–484 (1974).
29. Misra, B. & Sudarshan, E. C. G. The Zeno's paradox in quantum theory. *J. Math. Phys.* **18**, 756–763 (1977).
30. Itano, W. M., Heinzen, D. J., Bollinger, J. J. & Wineland, D. J. Quantum Zeno effect. *Phys. Rev. A* **41**, 2295–2300 (1990).
31. Lane, A. M. Decay at early times: larger or smaller than the golden rule? *Phys. Lett. A* **99**, 359–360 (1983).
32. Kofman, A. G. & Kurizki, G. Acceleration of quantum decay processes by frequent observations. *Nature* **405**, 546–550 (2000).
33. Harrington, P. M., Monroe, J. T. & Murch, K. W. Quantum Zeno effects from measurement controlled qubit-bath interactions. *Phys. Rev. Lett.* **118**, 240401 (2017).

34. Beige, A., Braun, D., Tregenna, B. & Knight, P. L. Quantum computing using dissipation to remain in a decoherence-free subspace. *Phys. Rev. Lett.* **85**, 1762–1765 (2000).
35. Facchi, P. & Pascazio, S. Quantum Zeno dynamics: mathematical and physical aspects. *J. Phys. A* **41**, 493001 (2008).
36. Facchi, P. & Pascazio, S. Quantum Zeno subspaces. *Phys. Rev. Lett.* **89**, 080401 (2002).
37. Lidar, D. A., Chuang, I. L. & Whaley, K. B. Decoherence-free subspaces for quantum computation. *Phys. Rev. Lett.* **81**, 2594–2597 (1998).
38. Hacohen-Gourgy, S., García-Pintos, L. P., Martin, L. S., Dressel, J. & Siddiqi, I. Incoherent qubit control using the quantum Zeno effect. *Phys. Rev. Lett.* **120**, 020505 (2018).
39. Sørensen, J. J. W. H., Dalgaard, M., Kiilerich, A. H., Mølmer, K. & Sherson, J. F. Quantum control with measurements and quantum Zeno dynamics. *Phys. Rev. A* **98**, 062317 (2018).
40. Mark, M. J. et al. Interplay between coherent and dissipative dynamics of bosonic doublons in an optical lattice. *Phys. Rev. Res.* **2**, 043050 (2020).
41. Raimond, J. M. et al. Phase space tweezers for tailoring cavity fields by quantum Zeno dynamics. *Phys. Rev. Lett.* **105**, 213601 (2010).
42. Raimond, J. M. et al. Quantum Zeno dynamics of a field in a cavity. *Phys. Rev. A* **86**, 032120 (2012).
43. Kumar, P., Snizhko, K., Gefen, Y. & Rosenow, B. Optimized steering: quantum state engineering and exceptional points. *Phys. Rev. A* **105**, L010203 (2022).
44. Snizhko, K., Kumar, P. & Romito, A. Quantum Zeno effect appears in stages. *Phys. Rev. Res.* **2**, 033512 (2020).
45. Zhu, B. et al. Suppressing the loss of ultracold molecules via the continuous quantum Zeno effect. *Phys. Rev. Lett.* **112**, 070404 (2014).
46. Chen, T. et al. Quantum Zeno effects across a parity-time symmetry breaking transition in atomic momentum space. *NPJ Quantum Inf.* https://doi.org/10.1038/s41534-021-00417-y (2021).
47. Ozawa, T. et al. Topological photonics. *Rev. Mod. Phys.* **91**, 015006 (2019).
48. Aliferis, P. & Preskill, J. Fault-tolerant quantum computation against biased noise. *Phys. Rev. A* **78**, 052331 (2008).
49. Shruti, P. et al. Bias-preserving gates with stabilized cat qubits. *Sci. Adv.* **6**, eaay5901 (2020).
50. Blumenthal, E. et al. Demonstration of universal control between non-interacting qubits using the Quantum Zeno effect. *npj Quantum Inf.* **8**, 88 (2022).
51. Shankar, S. et al. Autonomously stabilized entanglement between two superconducting quantum bits. *Nature* **504**, 419 (2013).
52. Murch, K. W. et al. Cavity-assisted quantum bath engineering. *Phys. Rev. Lett.* **109**, 183602 (2012).
53. Puri, S., Boutin, S. & Blais, A. Engineering the quantum states of light in a Kerr-nonlinear resonator by two-photon driving. *NPJ Quantum Inf.* **3**, 18 (2017).
54. Mamaev, M., Govia, L. C. G. & Clerk, A. A. Dissipative stabilization of entangled cat states using a driven Bose–Hubbard dimer. *Quantum* **2**, 58 (2018).
55. Krauter, H. et al. Entanglement generated by dissipation and steady state entanglement of two macroscopic objects. *Phys. Rev. Lett.* **107**, 080503 (2011).
56. Souquet, J.-R. & Clerk, A. A. Fock-state stabilization and emission in superconducting circuits using dc-biased Josephson junctions. *Phys. Rev. A* **93**, 060301 (2016).
57. Lin, Y. et al. Dissipative production of a maximally entangled steady state of two quantum bits. *Nature* **504**, 415–418 (2013).
58. Kienzler, D. et al. Quantum harmonic oscillator state synthesis by reservoir engineering. *Science* **347**, 53–56 (2015).
59. Plenio, M. B., Huelga, S. F., Beige, A. & Knight, P. L. Cavity-loss-induced generation of entangled atoms. *Phys. Rev. A* **59**, 2468–2475 (1999).
60. Kraus, B. et al. Preparation of entangled states by quantum Markov processes. *Phys. Rev. A* **78**, 042307 (2008).
61. Kastoryano, M. J., Reiter, F. & Sørensen, A. S. Dissipative preparation of entanglement in optical cavities. *Phys. Rev. Lett.* **106**, 090502 (2011).
62. Morigi, G. et al. Dissipative quantum control of a spin chain. *Phys. Rev. Lett.* **115**, 200502 (2015).
63. Ma, X., Viennot, J. J., Kotler, S., Teufel, J. D. & Lehnert, K. W. Non-classical energy squeezing of a macroscopic mechanical oscillator. *Nat. Phys.* **17**, 322–326 (2021).
64. Cole, D. C. et al. Resource-efficient dissipative entanglement of two trapped-ion qubits. *Phys. Rev. Lett.* **128**, 080502 (2022).
65. Aron, C., Kulkarni, M. & Türeci, H. E. Steady-state entanglement of spatially separated qubits via quantum bath engineering. *Phys. Rev. A* **90**, 062305 (2014).
66. Rao, D. D. B. & Mølmer, K. Deterministic entanglement of Rydberg ensembles by engineered dissipation. *Phys. Rev. A* **90**, 062319 (2014).
67. Martin, L., Sayrafi, M. & Whaley, K. B. What is the optimal way to prepare a Bell state using measurement and feedback? *Quantum Sci. Technol.* **2**, 044006 (2017).
68. Rao, D. D. B., Yang, S. & Wrachtrup, J. Dissipative entanglement of solid-state spins in diamond. *Phys. Rev. A* **95**, 022310 (2017).
69. Schuetz, M. J. A., Kessler, E. M., Vandersypen, L. M. K., Cirac, J. I. & Giedke, G. Nuclear spin dynamics in double quantum dots: multistability, dynamical polarization, criticality, and entanglement. *Phys. Rev. B* **89**, 195310 (2014).
70. Shao, X. Q., Wu, J. H. & Yi, X. X. Dissipation-based entanglement via quantum Zeno dynamics and Rydberg antiblockade. *Phys. Rev. A* **95**, 062339 (2017).
71. Didier, N., Guillaud, J., Shankar, S. & Mirrahimi, M. Remote entanglement stabilization and concentration by quantum reservoir engineering. *Phys. Rev. A* **98**, 012329 (2018).
72. Reiter, F., Reeb, D. & Sørensen, A. S. Scalable dissipative preparation of many-body entanglement. *Phys. Rev. Lett.* **117**, 040501 (2016).
73. Ma, S.-l., Li, X.-k., Liu, X.-y., Xie, J.-k. & Li, F.-l. Stabilizing Bell states of two separated superconducting qubits via quantum reservoir engineering. *Phys. Rev. A* **99**, 042336 (2019).
74. Sharma, V. & Mueller, E. J. Driven-dissipative control of cold atoms in tilted optical lattices. *Phys. Rev. A* **103**, 043322 (2021).
75. Colladay, K. R. & Mueller, E. J. Driven dissipative preparation of few-body Laughlin states of Rydberg polaritons in twisted cavities. Preprint at https://arxiv.org/abs/2107.06346 (2021).
76. Ticozzi, F. & Viola, L. Quantum Markovian subsystems: invariance, attractivity, and control. *IEEE Trans. Automat. Contr.* **53**, 2048–2063 (2008).
77. Braginskii, V., Manukin, A. & Tikhonov, M. Y. Investigation of dissipative ponderomotive effects of electromagnetic radiation. *J. Exp. Theor. Phys.* **31**, 829 (1970).
78. Cohadon, P. F., Heidmann, A. & Pinard, M. Cooling of a mirror by radiation pressure. *Phys. Rev. Lett.* **83**, 3174–3177 (1999).
79. Chan, J. et al. Laser cooling of a nanomechanical oscillator into its quantum ground state. *Nature* **478**, 89–92 (2011).
80. Rivière, R. et al. Optomechanical sideband cooling of a micromechanical oscillator close to the quantum ground state. *Phys. Rev. A* **83**, 063835 (2011).
81. Yong-Chun, L., Yu-Wen, H., Wei, W. C. & Yun-Feng, X. Review of cavity optomechanical cooling. *Chin. Phys. B* **22**, 114213 (2013).
82. Wineland, D. J. & Itano, W. M. Laser cooling. *Phys. Today* **40**, 34–40 (1987).
83. Hänsch, T. & Schawlow, A. Cooling of gases by laser radiation. *Opt. Commun.* **13**, 68–69 (1975).
84. Schreck, F. & Druten, K. V. Laser cooling for quantum gases. *Nat. Phys.* **17**, 1296–1304 (2021).
85. Phillips, W. D. Nobel lecture: laser cooling and trapping of neutral atoms. *Rev. Mod. Phys.* **70**, 721–741 (1998).
86. Stenholm, S. The semiclassical theory of laser cooling. *Rev. Mod. Phys.* **58**, 699–739 (1986).
87. Diedrich, F., Bergquist, J. C., Itano, W. M. & Wineland, D. J. Laser cooling to the zero-point energy of motion. *Phys. Rev. Lett.* **62**, 403–406 (1989).
88. Wiseman, H. M. & Milburn, G. J. All-optical versus electro-optical quantum-limited feedback. *Phys. Rev. A* **49**, 4110–4125 (1994).
89. Lloyd, S. Coherent quantum feedback. *Phys. Rev. A* **62**, 022108 (2000).
90. Zurek, W. H. Pointer basis of quantum apparatus: into what mixture does the wave packet collapse? *Phys. Rev. D* **24**, 1516–1525 (1981).
91. Jacobs, K. & Steck, D. A. A straightforward introduction to continuous quantum measurement. *Contemp. Phys.* **47**, 279–303 (2006).
92. Clerk, A. A., Devoret, M. H., Girvin, S. M., Marquardt, F. & Schoelkopf, R. J. Introduction to quantum noise, measurement, and amplification. *Rev. Mod. Phys.* **82**, 1155–1208 (2010).
93. Braginsky, V. B. & Khalili, F. Y. Quantum nondemolition measurements: the route from toys to tools. *Rev. Mod. Phys.* **68**, 1–11 (1996).
94. Wheeler, J. A. & Zurek, W. H. (eds) *Quantum Theory and Measurement* (Princeton Univ. Press, 2014); https://doi.org/10.1515/9781400854554
95. Hatridge, M. et al. Quantum back-action of an individual variable-strength measurement. *Science* **339**, 178–181 (2013).
96. Weber, S. J. et al. Mapping the optimal route between two quantum states. *Nature* **511**, 570–573 (2014).
97. Campagne-Ibarcq, P. et al. Observing quantum state diffusion by heterodyne detection of fluorescence. *Phys. Rev. X* **6**, 011002 (2016).
98. Hacohen-Gourgy, S. et al. Quantum dynamics of simultaneously measured non-commuting observables. *Nature* **538**, 491–494 (2016).
99. Flurin, E., Martin, L. S., Hacohen-Gourgy, S. & Siddiqi, I. Using a recurrent neural network to reconstruct quantum dynamics of a superconducting qubit from physical observations. *Phys. Rev. X* **10**, 011006 (2020).
100. Lloyd, S. & Viola, L. Engineering quantum dynamics. *Phys. Rev. A* **65**, 010101 (2001).
101. Herasymenko, Y., Gornyi, I. & Gefen, Y. Measurement-driven navigation in many-body Hilbert space: active-decision steering. Preprint at https://arxiv.org/abs/2111.09306 (2021).
102. Wiseman, H. M. & Milburn, G. J. *Quantum Measurement and Control* (Cambridge Univ. Press, 2009).
103. Martin, L. S., Livingston, W. P., Hacohen-Gourgy, S., Wiseman, H. M. & Siddiqi, I. Implementation of a canonical phase measurement with quantum feedback. *Nat. Phys.* **16**, 1046–1049 (2020).
104. Gertler, J. M. et al. Protecting a bosonic qubit with autonomous quantum error correction. *Nature* **590**, 243–248 (2021).
105. Ahn, C., Doherty, A. C. & Landahl, A. J. Continuous quantum error correction via quantum feedback control. *Phys. Rev. A* **65**, 042301 (2002).
106. Atalaya, J. et al. Continuous quantum error correction for evolution under time-dependent Hamiltonians. *Phys. Rev. A* **103**, 042406 (2021).
107. Kerckhoff, J., Nurdin, H. I., Pavlichin, D. S. & Mabuchi, H. Designing quantum memories with embedded control: photonic circuits for autonomous quantum error correction. *Phys. Rev. Lett.* **105**, 040502 (2010).
108. Kapit, E. Hardware-efficient and fully autonomous quantum error correction in superconducting circuits. *Phys. Rev. Lett.* **116**, 150501 (2016).
109. Reiter, F., Sørensen, A. S., Zoller, P. & Muschik, C. A. Dissipative quantum error correction and application to quantum sensing with trapped ions. *Nat. Commun.* **8**, 1822 (2017).
110. Albert, V. V. et al. Pair-cat codes: autonomous error-correction with low-order nonlinearity. *Quantum Sci. Technol.* **4**, 035007 (2019).
111. Sarovar, M. & Milburn, G. J. Continuous quantum error correction by cooling. *Phys. Rev. A* **72**, 012306 (2005).
112. de Neeve, B. & Nguyen, T.-L. & Behrle, T. & Home, J. P. Error correction of a logical grid state qubit by dissipative pumping. *Nat. Phys* **18**, 296300 (2022).
113. Kristensen, L. B., Kjaergaard, M., Andersen, C. K. & Zinner, N. T. Hybrid quantum error correction in qubit architectures. Preprint at https://arxiv.org/abs/1909.09112 (2019).
114. Lihm, J.-M., Noh, K. & Fischer, U. R. Implementation-independent sufficient condition of the Knill–Laflamme type for the autonomous protection of logical qudits by strong engineered dissipation. *Phys. Rev. A* **98**, 012317 (2018).
115. Gyenis, A. et al. Moving beyond the transmon: noise-protected superconducting quantum circuits. *PRX Quantum* **2**, 030101 (2021).
116. Peres, A. Reversible logic and quantum computers. *Phys. Rev. A* **32**, 3266–3276 (1985).
117. Bultink, C. C. et al. Protecting quantum entanglement from leakage and qubit errors via repetitive parity measurements. *Sci. Adv.* **6**, eaay3050 (2020).
118. Fowler, A. G., Mariantoni, M., Martinis, J. M. & Cleland, A. N. Surface codes: towards practical large-scale quantum computation. *Phys. Rev. A* **86**, 032324 (2012).
119. Córcoles, A. et al. Demonstration of a quantum error detection code using a square lattice of four superconducting qubits. *Nat. Commun*. https://doi.org/10.1038/ncomms7979 (2015).
120. Versluis, R. et al. Scalable quantum circuit and control for a superconducting surface code. *Phys. Rev. Appl.* **8**, 034021 (2017).
121. Cai, W., Ma, Y., Wang, W., Zou, C.-L. & Sun, L. Bosonic quantum error correction codes in superconducting quantum circuits. *Fundam. Res.* **1**, 50–67 (2021).

122. Michael, M. H. et al. New class of quantum error-correcting codes for a bosonic mode. *Phys. Rev. X* **6**, 031006 (2016).
123. Axline, C. J. et al. On-demand quantum state transfer and entanglement between remote microwave cavity memories. *Nat. Phys.* **14**, 705–710 (2018).
124. Mirrahimi, M. et al. Dynamically protected cat-qubits: a new paradigm for universal quantum computation. *New J. Phys.* **16**, 045014 (2014).
125. Guillaud, J. & Mirrahimi, M. Repetition cat qubits for fault-tolerant quantum computation. *Phys. Rev. X* **9**, 041053 (2019).
126. Grimm, A. et al. Stabilization and operation of a Kerr-cat qubit. *Nature* **584**, 205–209 (2020).
127. Tóth, L. D., Bernier, N. R., Nunnenkamp, A., Feofanov, A. K. & Kippenberg, T. J. A dissipative quantum reservoir for microwave light using a mechanical oscillator. *Nat. Phys.* **13**, 787–793 (2017).
128. Ofek, N. et al. Extending the lifetime of a quantum bit with error correction in superconducting circuits. *Nature* **536**, 441–445 (2016).
129. Hu, L. et al. Quantum error correction and universal gate set operation on a binomial bosonic logical qubit. *Nat. Phys.* **15**, 503–508 (2019).
130. Gottesman, D., Kitaev, A. & Preskill, J. Encoding a qubit in an oscillator. *Phys. Rev. A* **64**, 012310 (2001).
131. Campagne-Ibarcq, P. et al. Quantum error correction of a qubit encoded in grid states of an oscillator. *Nature* **584**, 368–372 (2020).
132. Flühmann, C. et al. Encoding a qubit in a trapped-ion mechanical oscillator. *Nature* **566**, 513–517 (2019).
133. Livingston, W. P. et al. Experimental demonstration of continuous quantum error correction. *Nat. Commun.* **13**, 2307 (2022).
134. Minev, Z. K. et al. To catch and reverse a quantum jump mid-flight. *Nature* **570**, 200–204 (2019).
135. Degen, C. L., Reinhard, F. & Cappellaro, P. Quantum sensing. *Rev. Mod. Phys.* **89**, 035002 (2017).
136. Maze, J. R. et al. Nanoscale magnetic sensing with an individual electronic spin in diamond. *Nature* **455**, 644–647 (2008).
137. Balasubramanian, G. et al. Nanoscale imaging magnetometry with diamond spins under ambient conditions. *Nature* **455**, 648–651 (2008).
138. Kolkowitz, S. et al. Probing Johnson noise and ballistic transport in normal metals with a single-spin qubit. *Science* **347**, 1129–1132 (2015).
139. Zu, C. et al. Emergent hydrodynamics in a strongly interacting dipolar spin ensemble. *Nature* **597**, 45–50 (2021).
140. Serniak, K. et al. Direct dispersive monitoring of charge parity in offset-charge-sensitive transmons. *Phys. Rev. Appl.* **12**, 014052 (2019).
141. Braginsky, V. B., Vorontsov, Y. I. & Thorne, K. S. Quantum nondemolition measurements. *Science* **209**, 547–557 (1980).
142. Lupaşcu, A. et al. Quantum non-demolition measurement of a superconducting two-level system. *Nat. Phys.* **3**, 119–123 (2007).
143. Xie, Y. et al. Dissipative quantum sensing with a magnetometer based on nitrogen-vacancy centers in diamond. *Phys. Rev. Appl.* **14**, 014013 (2020).
144. Khanahmadi, M. & Mølmer, K. Time-dependent atomic magnetometry with a recurrent neural network. *Phys. Rev. A* **103**, 032406 (2021).
145. Nolan, S. P., Smerzi, A. & Pezzè, L. A machine learning approach to Bayesian parameter estimation. Preprint at https://arxiv.org/abs/2006.02369 (2021).
146. Altman, E. et al. Quantum simulators: architectures and opportunities. *PRX Quantum* **2**, 017003 (2021).
147. Blatt, R. & Roos, C. F. Quantum simulations with trapped ions. *Nat. Phys.* **8**, 277–284 (2012).
148. Aspuru-Guzik, A. & Walther, P. Photonic quantum simulators. *Nat. Phys.* **8**, 285–291 (2012).
149. Gross, C. & Bloch, I. Quantum simulations with ultracold atoms in optical lattices. *Science* **357**, 995–1001 (2017).
150. Houck, A. A., Türeci, H. E. & Koch, J. On-chip quantum simulation with superconducting circuits. *Nat. Phys.* **8**, 292–299 (2012).
151. Schäfer, F., Fukuhara, T., Sugawa, S., Takasu, Y. & Takahashi, Y. Tools for quantum simulation with ultracold atoms in optical lattices. *Nat. Rev. Phys.* **2**, 411–425 (2020).
152. Noh, C. & Angelakis, D. G. Quantum simulations and many-body physics with light. *Rep. Progr. Phys.* **80**, 016401 (2016).
153. Georgescu, I. M., Ashhab, S. & Nori, F. Quantum simulation. *Rev. Mod. Phys.* **86**, 153–185 (2014).
154. Poplavskii, R. P. Thermodynamic models of information processes. *Phys. Usp.* **18**, 222–241 (1975).
155. Manin, Y. I. Vychislimoe i nevychislimoe [Computable and uncomputable]. *Sov. Radio Moscow* 13–15 (1980).
156. Feynman, R. P. Simulating physics with computers. *Int. J. Theor. Phys.* **21**, 467–488 (1982).
157. Feynman, R. P. Quantum mechanical computers. *Opt. News* **11**, 11–20 (1985).
158. Weimer, H., Müller, M., Lesanovsky, I., Zoller, P. & Büchler, H. P. A Rydberg quantum simulator. *Nat. Phys.* **6**, 382–388 (2010).
159. Bernien, H. et al. Probing many-body dynamics on a 51-atom quantum simulator. *Nature* **551**, 579–584 (2017).
160. Barreiro, J. T. et al. An open-system quantum simulator with trapped ions. *Nature* **470**, 486–491 (2011).
161. Kollár, A. J., Fitzpatrick, M. & Houck, A. A. Hyperbolic lattices in circuit quantum electrodynamics. *Nature* **571**, 45–50 (2019).
162. Hoening, M., Abdussalam, W., Fleischhauer, M. & Pohl, T. Antiferromagnetic long-range order in dissipative Rydberg lattices. *Phys. Rev. A* **90**, 021603 (2014).
163. Sieberer, L. M., Buchhold, M. & Diehl, S. Keldysh field theory for driven open quantum systems. *Rep. Progr. Phys.* **79**, 096001 (2016).
164. Foss-Feig, M. et al. Emergent equilibrium in many-body optical bistability. *Phys. Rev. A* **95**, 043826 (2017).
165. Cao, Y. et al. Quantum chemistry in the age of quantum computing. *Chem. Rev.* **119**, 10856–10915 (2019).
166. Reiher, M., Wiebe, N., Svore, K. M., Wecker, D. & Troyer, M. Elucidating reaction mechanisms on quantum computers. *Proc. Natl Acad. Sci. USA* **114**, 7555–7560 (2017).
167. O'Malley, P. J. J. et al. Scalable quantum simulation of molecular energies. *Phys. Rev. X* **6**, 031007 (2016).
168. Dorner, R., Goold, J. & Vedral, V. Towards quantum simulations of biological information flow. *Interface Focus* **2**, 522–528 (2012).
169. Ribeiro, H. & Marquardt, F. Kinetics of many-body reservoir engineering. *Phys. Rev. Res.* **2**, 033231 (2020).
170. Wang, H. Quantum algorithm for preparing the ground state of a system via resonance transition. *Sci. Rep.* https://doi.org/10.1038/s41598-017-16396-0 (2017).
171. Sharma, V. & Mueller, E. J. Driven-dissipative control of cold atoms in tilted optical lattices. *Phys. Rev. A* **103**, 043322 (2021).
172. Zhou, L., Choi, S. & Lukin, M. D. Symmetry-protected dissipative preparation of matrix product states. *Phys. Rev. A* **104**, 032418 (2021).
173. Kjaergaard, M. et al. Superconducting qubits: current state of play. *Annu. Rev. Condens. Matter Phys.* **11**, 369–395 (2020).
174. Roy, S., Chalker, J. T., Gornyi, I. V. & Gefen, Y. Measurement-induced steering of quantum systems. *Phys. Rev. Res.* **2**, 033347 (2020).
175. Ramos, T., Pichler, H., Daley, A. J. & Zoller, P. Quantum spin dimers from chiral dissipation in cold-atom chains. *Phys. Rev. Lett.* **113**, 237203 (2014).
176. Das, A. & Chakrabarti, B. K. Colloquium: Quantum annealing and analog quantum computation. *Rev. Mod. Phys.* **80**, 1061–1081 (2008).
177. Stormer, H. L., Tsui, D. C. & Gossard, A. C. The fractional quantum Hall effect. *Rev. Mod. Phys.* **71**, S298–S305 (1999).
178. Moore, G. & Read, N. Nonabelions in the fractional quantum Hall effect. *Nucl. Phys. B* **360**, 362–396 (1991).
179. Roncaglia, M., Rizzi, M. & Cirac, J. I. Pfaffian state generation by strong three-body dissipation. *Phys. Rev. Lett.* **104**, 096803 (2010).
180. Daley, A. J., Taylor, J. M., Diehl, S., Baranov, M. & Zoller, P. Atomic three-body loss as a dynamical three-body interaction. *Phys. Rev. Lett.* **102**, 040402 (2009).
181. Diehl, S., Baranov, M., Daley, A. J. & Zoller, P. Quantum field theory for the three-body constrained lattice Bose gas. I. Formal developments. *Phys. Rev. B* **82**, 064509 (2010).
182. Diehl, S., Baranov, M., Daley, A. J. & Zoller, P. Quantum field theory for the three-body constrained lattice Bose gas. II. Application to the many-body problem. *Phys. Rev. B* **82**, 064510 (2010).
183. Dogra, N. et al. Dissipation-induced structural instability and chiral dynamics in a quantum gas. *Science* **366**, 1496–1499 (2019).
184. Zundel, L. A. et al. Energy-dependent three-body loss in 1D Bose gases. *Phys. Rev. Lett.* **122**, 013402 (2019).
185. Bonnes, L. & Wessel, S. Pair superfluidity of three-body constrained bosons in two dimensions. *Phys. Rev. Lett.* **106**, 185302 (2011).
186. Syassen, N. et al. Strong dissipation inhibits losses and induces correlations in cold molecular gases. *Science* **320**, 1329–1331 (2008).
187. Fröml, H., Muckel, C., Kollath, C., Chiocchetta, A. & Diehl, S. Ultracold quantum wires with localized losses: many-body quantum Zeno effect. *Phys. Rev. B* **101**, 144301 (2020).
188. Tomita, T., Nakajima, S., Takasu, Y. & Takahashi, Y. Dissipative Bose–Hubbard system with intrinsic two-body loss. *Phys. Rev. A* **99**, 031601 (2019).
189. Dürr, S. et al. Lieb–Liniger model of a dissipation-induced Tonks–Girardeau gas. *Phys. Rev. A* **79**, 023614 (2009).
190. Ramos, T., Pichler, H., Daley, A. J. & Zoller, P. Quantum spin dimers from chiral dissipation in cold-atom chains. *Phys. Rev. Lett.* **113**, 237203 (2014).
191. Bañuls, M. C. et al. Simulating lattice gauge theories within quantum technologies. *Eur. Phys. J. D* **74**, 165 (2020).
192. Stannigel, K. et al. Constrained dynamics via the Zeno effect in quantum simulation: implementing non-Abelian lattice gauge theories with cold atoms. *Phys. Rev. Lett.* **112**, 120406 (2014).
193. Caballar, R. C. F., Diehl, S., Mäkelä, H., Oberthaler, M. & Watanabe, G. Dissipative preparation of phase- and number-squeezed states with ultracold atoms. *Phys. Rev. A* **89**, 013620 (2014).
194. Carusotto, I. et al. Photonic materials in circuit quantum electrodynamics. *Nat. Phys.* **16**, 268–279 (2020).
195. Schmitt, J. et al. Observation of grand-canonical number statistics in a photon Bose–Einstein condensate. *Phys. Rev. Lett.* **112**, 030401 (2014).
196. Hafezi, M., Adhikari, P. & Taylor, J. M. Chemical potential for light by parametric coupling. *Phys. Rev. B* **92**, 174305 (2015).
197. Verstraete, F., Wolf, M. M. & Cirac, I. J. Quantum computation and quantum-state engineering driven by dissipation. *Nat. Phys.* **5**, 633–636 (2009).
198. Jaschke, D., Montangero, S. & Carr, L. D. One-dimensional many-body entangled open quantum systems with tensor network methods. *Quantum Sci. Technol.* **4**, 013001 (2018).
199. Yanay, Y. & Clerk, A. A. Reservoir engineering of bosonic lattices using chiral symmetry and localized dissipation. *Phys. Rev. A* **98**, 043615 (2018).
200. Diehl, S. et al. Quantum states and phases in driven open quantum systems with cold atoms. *Nat. Phys.* **4**, 878–883 (2008).
201. Diehl, S., Rico, E., Baranov, M. A. & Zoller, P. Topology by dissipation in atomic quantum wires. *Nat. Phys.* **7**, 971–977 (2011).
202. Cian, Z.-P. et al. Photon pair condensation by engineered dissipation. *Phys. Rev. Lett.* **123**, 063602 (2019).
203. Bardyn, C.-E. et al. Topology by dissipation. *New J. Phys.* **15**, 085001 (2013).
204. Shavit, G. & Goldstein, M. Topology by dissipation: transport properties. *Phys. Rev. B* **101**, 125412 (2020).
205. Goldstein, M. Dissipation-induced topological insulators: a no-go theorem and a recipe. *SciPost Phys.* **7**, 67 (2019).
206. Iemini, F., Rossini, D., Fazio, R., Diehl, S. & Mazza, L. Dissipative topological superconductors in number-conserving systems. *Phys. Rev. B* **93**, 115113 (2016).
207. Dangel, F., Wagner, M., Cartarius, H., Main, J. & Wunner, G. Topological invariants in dissipative extensions of the Su–Schrieffer–Heeger model. *Phys. Rev. A* **98**, 013628 (2018).
208. Barbarino, S., Yu, J., Zoller, P. & Budich, J. C. Preparing atomic topological quantum matter by adiabatic nonunitary dynamics. *Phys. Rev. Lett.* **124**, 010401 (2020).
209. Kitaev, A. & Laumann, C. Topological phases and quantum computation. In *Exact Methods in Low-dimensional Statistical Physics and Quantum Computing. Lecture Notes of the Les Houches Summer School Vol. 89* (eds Jacobsen, J. et al.) 101–125 (Oxford Univ. Press, 2010).
210. Pincus, M. A Monte Carlo method for the approximate solution of certain types of constrained optimization problems. *Oper. Res.* **18**, 1225–1228 (1970).
211. Bishop, C. *Pattern Recognition and Machine Learning* (Springer, 2006).
212. Chen, D., Meldgin, C. & DeMarco, B. Bath-induced band decay of a Hubbard lattice gas. *Phys. Rev. A* **90**, 013602 (2014).
213. Lena, R. G. & Daley, A. J. Dissipative dynamics and cooling rates of trapped impurity atoms immersed in a reservoir gas. *Phys. Rev. A* **101**, 033612 (2020).
214. McKay, D. C., Meldgin, C., Chen, D. & DeMarco, B. Slow thermalization between a lattice and free Bose gas. *Phys. Rev. Lett.* **111**, 063002 (2013).
215. Shabani, A. & Neven, H. Artificial quantum thermal bath: engineering temperature for a many-body quantum system. *Phys. Rev. A* **94**, 052301 (2016).

216. Metcalf, M., Moussa, J. E., de Jong, W. A. & Sarovar, M. Engineered thermalization and cooling of quantum many-body systems. *Phys. Rev. Res.* **2**, 023214 (2020).
217. Su, H.-Y. & Li, Y. Quantum algorithm for the simulation of open-system dynamics and thermalization. *Phys. Rev. A* **101**, 012328 (2020).
218. Schönleber, D. W., Bentley, C. D. B. & Eisfeld, A. Engineering thermal reservoirs for ultracold dipole–dipole-interacting Rydberg atoms. *New J. Phys.* **20**, 013011 (2018).
219. Dive, B., Mintert, F. & Burgarth, D. Quantum simulations of dissipative dynamics: time dependence instead of size. *Phys. Rev. A* **92**, 032111 (2015).
220. Griessner, A., Daley, A. J., Clark, S. R., Jaksch, D. & Zoller, P. Dissipative dynamics of atomic Hubbard models coupled to a phonon bath: dark state cooling of atoms within a Bloch band of an optical lattice. *New J. Phys.* **9**, 44–44 (2007).
221. Yanay, Y. & Clerk, A. A. Reservoir engineering with localized dissipation: dynamics and prethermalization. *Phys. Rev. Res.* **2**, 023177 (2020).
222. Liu, Y.-C., Hu, Y.-W., Wong, C. W. & Xiao, Y.-F. Review of cavity optomechanical cooling. *Chin. Phys. B* **22**, 114213 (2013).
223. Letokhov, V. S., Ol'shanii, M. A. & Ovchinnikov, Y. B. Laser cooling of atoms: a review. *Quantum Semiclass. Opt.* **7**, 5–40 (1995).
224. Marquardt, F., Clerk, A. & Girvin, S. Quantum theory of optomechanical cooling. *J. Mod. Opt.* **55**, 3329–3338 (2008).
225. McKay, D. C. & DeMarco, B. Cooling in strongly correlated optical lattices: prospects and challenges. *Rep. Progr. Phys.* **74**, 054401 (2011).
226. Guo, J., Norte, R. & Gröblacher, S. Feedback cooling of a room temperature mechanical oscillator close to its motional ground state. *Phys. Rev. Lett.* **123**, 223602 (2019).
227. Shen, C. et al. Quantum channel construction with circuit quantum electrodynamics. *Phys. Rev. B* **95**, 134501 (2017).
228. Di Candia, R., Pedernales, J. S., del Campo, A., Solano, E. & Casanova, J. Quantum simulation of dissipative processes without reservoir engineering. *Sci. Rep.* **5**, 9981 (2015).
229. Chenu, A., Beau, M., Cao, J. & del Campo, A. Quantum simulation of generic many-body open system dynamics using classical noise. *Phys. Rev. Lett.* **118**, 140403 (2017).
230. Sweke, R., Sinayskiy, I., Bernard, D. & Petruccione, F. Universal simulation of Markovian open quantum systems. *Phys. Rev. A* **91**, 062308 (2015).
231. Zanardi, P., Marshall, J. & Campos Venuti, L. Dissipative universal Lindbladian simulation. *Phys. Rev. A* **93**, 022312 (2016).
232. Carmele, A., Knorr, A. & Milde, F. Stabilization of photon collapse and revival dynamics by a non-Markovian phonon bath. *New J. Phys.* **15**, 105024 (2013).
233. Lebreuilly, J. et al. Stabilizing strongly correlated photon fluids with non-Markovian reservoirs. *Phys. Rev. A* **96**, 033828 (2017).
234. Cai, Z., Schollwöck, U. & Pollet, L. Identifying a bath-induced Bose liquid in interacting spin-boson models. *Phys. Rev. Lett.* **113**, 260403 (2014).
235. Maghrebi, M. F. & Gorshkov, A. V. Nonequilibrium many-body steady states via Keldysh formalism. *Phys. Rev. B* **93**, 014307 (2016).
236. Hurst, H. M., Guo, S. & Spielman, I. B. Feedback induced magnetic phases in binary Bose–Einstein condensates. *Phys. Rev. Research* **2**, 043325 (2020).
237. Tomita, T., Nakajima, S., Danshita, I., Takasu, Y. & Takahashi, Y. Observation of the Mott insulator to superfluid crossover of a driven-dissipative Bose–Hubbard system. *Sci. Adv.* https://advances.sciencemag.org/content/3/12/e1701513 (2017).
238. Rylands, C., Guo, Y., Lev, B. L., Keeling, J. & Galitski, V. Photon-mediated Peierls transition of a 1D gas in a multimode optical cavity. *Phys. Rev. Lett.* **125**, 010404 (2020).
239. Sieberer, L. M., Huber, S. D., Altman, E. & Diehl, S. Dynamical critical phenomena in driven-dissipative systems. *Phys. Rev. Lett.* **110**, 195301 (2013).
240. Essink, S., Wolff, S., Schütz, G. M., Kollath, C. & Popkov, V. Transition between dissipatively stabilized helical states. *Phys. Rev. Res.* **2**, 022007 (2020).
241. Scarlatella, O., Fazio, R. & Schirò, M. Emergent finite frequency criticality of driven-dissipative correlated lattice bosons. *Phys. Rev. B* **99**, 064511 (2019).
242. Mathey, S. & Diehl, S. Absence of criticality in the phase transitions of open Floquet systems. *Phys. Rev. Lett.* **122**, 110602 (2019).
243. Brennecke, F. et al. Real-time observation of fluctuations at the driven-dissipative Dicke phase transition. *Proc. Natl Acad. Sci. USA* **110**, 11763–11767 (2013).
244. Foss-Feig, M. et al. Emergent equilibrium in many-body optical bistability. *Phys. Rev. A* **95**, 043826 (2017).
245. Fitzpatrick, M., Sundaresan, N. M., Li, A. C. Y., Koch, J. & Houck, A. A. Observation of a dissipative phase transition in a one-dimensional circuit QED lattice. *Phys. Rev. X* **7**, 011016 (2017).
246. Else, D. V., Monroe, C., Nayak, C. & Yao, N. Y. Discrete time crystals. *Annu. Rev. Condens. Matter Phys.* **11**, 467–499 (2020).
247. Sacha, K. & Zakrzewski, J. Time crystals: a review. *Rep. Progr. Phys.* **81**, 016401 (2017).
248. Riera-Campeny, A., Moreno-Cardoner, M. & Sanpera, A. Time crystallinity in open quantum systems. *Quantum* **4**, 270 (2020).
249. Buča, B., Tindall, J. & Jaksch, D. Non-stationary coherent quantum many-body dynamics through dissipation. *Nat. Commun.* **10**, 1730 (2019).
250. Marais, A. et al. The future of quantum biology. *J. R. Soc. Interface* **15**, 20180640 (2018).
251. Fujii, K. & Nakajima, K. Harnessing disordered-ensemble quantum dynamics for machine learning. *Phys. Rev. Appl.* **8**, 024030 (2017).
252. Angelatos, G., Khan, S. A. & Türeci, H. E. Reservoir computing approach to quantum state measurement. *Phys. Rev. X* **11**, 041062 (2021).
253. Carroll, T. L. Optimizing memory in reservoir computers. *Chaos* **32**, 023123 (2022).
254. Koch, J. et al. Charge-insensitive qubit design derived from the Cooper pair box. *Phys. Rev. A* **76**, 042319 (2007).
255. Manucharyan, V. E., Koch, J., Glazman, L. I. & Devoret, M. H. Fluxonium: single Cooper-pair circuit free of charge offsets. *Science* **326**, 113–116 (2009).
256. Gyenis, A. et al. Moving beyond the transmon: noise-protected superconducting quantum circuits. *PRX Quantum* **2**, 030101 (2021).
257. Deffner, S. & Campbell, S. *Quantum Thermodynamics*, 2053–2571 (Morgan & Claypool, 2019); https://doi.org/10.1088/2053-2571/ab21c6
258. Vinjanampathy, S. & Anders, J. Quantum thermodynamics. *Contemp. Phys.* **57**, 545–579 (2016).
259. Polkovnikov, A., Sengupta, K., Silva, A. & Vengalattore, M. Colloquium: nonequilibrium dynamics of closed interacting quantum systems. *Rev. Mod. Phys.* **83**, 863–883 (2011).
260. Maldacena, J., Shenker, S. H. & Stanford, D. A bound on chaos. *J. High Energy Phys.* **2016**, 106 (2016).
261. Nahum, A., Vijay, S. & Haah, J. Operator spreading in random unitary circuits. *Phys. Rev. X* **8**, 021014 (2018).
262. Li, Y. & Fisher, M. P. A. Statistical mechanics of quantum error correcting codes. *Phys. Rev. B* **103**, 104306 (2021).
263. D'Alessio, L., Kafri, Y., Polkovnikov, A. & Rigol, M. From quantum chaos and eigenstate thermalization to statistical mechanics and thermodynamics. *Adv. Phys.* **65**, 239–362 (2016).
264. Luitz, D. J. & Bar Lev, Y. Information propagation in isolated quantum systems. *Phys. Rev. B* **96**, 020406 (2017).
265. Chan, A., Nandkishore, R. M., Pretko, M. & Smith, G. Unitary-projective entanglement dynamics. *Phys. Rev. B* **99**, 224307 (2019).
266. Li, Y., Chen, X. & Fisher, M. P. A. Measurement-driven entanglement transition in hybrid quantum circuits. *Phys. Rev. B* **100**, 134306 (2019).
267. Skinner, B., Ruhman, J. & Nahum, A. Measurement-induced phase transitions in the dynamics of entanglement. *Phys. Rev. X* **9**, 031009 (2019).
268. Ippoliti, M., Gullans, M. J., Gopalakrishnan, S., Huse, D. A. & Khemani, V. Entanglement phase transitions in measurement-only dynamics. *Phys. Rev. X* **11**, 011030 (2021).
269. Marino, J. Universality class of Ising critical states with long-range losses. Preprint at https://arxiv.org/abs/2108.12422 (2021).
270. Deutsch, J. M. Quantum statistical mechanics in a closed system. *Phys. Rev. A* **43**, 2046–2049 (1991).
271. Nandkishore, R. & Huse, D. A. Many-body localization and thermalization in quantum statistical mechanics. *Annu. Rev. Condens. Matter Phys.* **6**, 15–38 (2015).
272. Abanin, D. A., Altman, E., Bloch, I. & Serbyn, M. Colloquium: Many-body localization, thermalization, and entanglement. *Rev. Mod. Phys.* **91**, 021001 (2019).
273. Khemani, V., Vishwanath, A. & Huse, D. A. Operator spreading and the emergence of dissipative hydrodynamics under unitary evolution with conservation laws. *Phys. Rev. X* **8**, 031057 (2018).
274. Valdez, M. A., Jaschke, D., Vargas, D. L. & Carr, L. D. Quantifying complexity in quantum phase transitions via mutual information complex networks. *Phys. Rev. Lett.* **119**, 225301 (2017).
275. Walschaers, M., Treps, N., Sundar, B., Carr, L. D. & Parigi, V. Emergent complex quantum networks in continuous-variables non-Gaussian states. Preprint at https://arxiv.org/abs/2012.15608 (2021).
276. Zwolak, M. & Vidal, G. Mixed-state dynamics in one-dimensional quantum lattice systems: a time-dependent superoperator renormalization algorithm. *Phys. Rev. Lett.* **93**, 207205 (2004).
277. Cui, J., Cirac, J. I. & Bañuls, M. C. Variational matrix product operators for the steady state of dissipative quantum systems. *Phys. Rev. Lett.* **114**, 220601 (2015).
278. Nagy, A. & Savona, V. Variational quantum Monte Carlo method with a neural-network ansatz for open quantum systems. *Phys. Rev. Lett.* **122**, 250501 (2019).
279. Hartmann, M. J. & Carleo, G. Neural-network approach to dissipative quantum many-body dynamics. *Phys. Rev. Lett.* **122**, 250502 (2019).
280. Vicentini, F., Biella, A., Regnault, N. & Ciuti, C. Variational neural-network ansatz for steady states in open quantum systems. *Phys. Rev. Lett.* **122**, 250503 (2019).
281. Yoshioka, N. & Hamazaki, R. Constructing neural stationary states for open quantum many-body systems. *Phys. Rev. B* **99**, 214306 (2019).
282. Liu, Z., Duan, L.-M. & Deng, D.-L. Solving quantum master equations with deep quantum neural networks. *Phys. Rev. Res.* **4**, 013097 (2022).
283. de Vega, I. & Alonso, D. Dynamics of non-Markovian open quantum systems. *Rev. Mod. Phys.* **89**, 015001 (2017).
284. Vacchini, B. *Frontiers of Open Quantum System Dynamics*, 71–85 (Springer, 2019); https://doi.org/10.1007/978-3-030-06122-7_4
285. Braunstein, S. L. & Caves, C. M. Statistical distance and the geometry of quantum states. *Phys. Rev. Lett.* **72**, 3439–3443 (1994).
286. Wootters, W. K. Statistical distance and Hilbert space. *Phys. Rev. D* **23**, 357–362 (1981).
287. Breuer, H.-P. & Petruccione, F. *The Theory of Open Quantum Systems* (Oxford Univ. Press, 2007).
288. Naghiloo, M., Abbasi, M., Joglekar, Y. N. & Murch, K. W. Quantum state tomography across the exceptional point in a single dissipative qubit. *Nat. Phys.* **15**, 1232–1236 (2019).
289. El-Ganainy, R. et al. Non-Hermitian physics and PT symmetry. *Nat. Phys.* **14**, 11–19 (2018).
290. Kraus, K., Böhm, A., Dollard, J. D. & Wootters, W. H. *States, Effects, and Operations: Fundamental Notions of Quantum Theory* (Springer, 1983).

Acknowledgements
We thank M. Hays, P. McMahon, A. Di Paulo and Y. Yanay for critical comments. This research was supported by an appointment to the Intelligence Community Postdoctoral Research Fellowship Program at MIT, administered by Oak Ridge Institute for Science and Education through an interagency agreement between the US Department of Energy and the Office of the Director of National Intelligence. This material is based upon work supported by the National Science Foundation under grant no. PHY-2110250, no. PHY-1752844 (CAREER), and a New Frontier Grant awarded by the College of Arts and Sciences at Cornell.

Author contributions
The authors contributed equally to all aspects of the article.

Competing interests
The authors declare no competing interests.

Peer review information
Nature Reviews Physics thanks the anonymous reviewers for their contribution to the peer review of this work.

Publisher's note
Springer Nature remains neutral with regard to jurisdictional claims in published maps and institutional affiliations.

Springer Nature or its licensor holds exclusive rights to this article under a publishing agreement with the author(s) or other rightsholder(s); author self-archiving of the accepted manuscript version of this article is solely governed by the terms of such publishing agreement and applicable law.

© Springer Nature Limited 2022